

Biomarker identification of thyroid associated ophthalmopathy using microarray data

Hong-Bin Yang¹, Jie Jiang¹, Lu-Lu Li², Huang-Qiang Yang², Xiao-Yu Zhang²

¹Department of Ophthalmology, the First Affiliated Hospital of Harbin Medical University, Harbin 150080, Heilongjiang Province, China

²Department of Neurosurgery, the Second Affiliated Hospital of Harbin Medical University, Harbin 150080, Heilongjiang Province, China

Correspondence to: Xiao-Yu Zhang. Department of Neurosurgery, the Second Affiliated Hospital of Harbin Medical University, No. 246 Xuefu Road, Nangang District, Harbin 150080, Heilongjiang Province, China. YuzhouZ88@163.com
Received: 2017-09-05 Accepted: 2018-01-03

Abstract

• **AIM:** To uncover the underlying pathogenesis of thyroid associated ophthalmopathy (TAO) and explore potential biomarkers of this disease.

• **METHODS:** The expression profile GSE9340, which was downloaded from Gene Expression Omnibus database, included 18 specimens from 10 TAO patients and 8 hyperthyroidism patients without ophthalmopathy. The platform was HumanRef-8 v2 Expression BeadChip. Raw data were normalized using preprocess. Core package and the differentially expressed genes (DEGs) were identified based on *t*-test with limma package of R. Functional enrichment analyses were performed recruiting the DAVID tool. Based on STRING database, a protein-protein interaction (PPI) network was constructed, from which a module was extracted. The functional enrichment for genes in the module was performed by the BinGO plugin.

• **RESULTS:** In total, 861 DEGs (433 up-regulated and 428 down-regulated) between TAO patients and hyperthyroidism patients without ophthalmopathy were identified. Crucial nodes in the PPI network included TPX2, CDCA5, PRC1, KIF23 and MKI67, which were also remarkable in the module and all enriched in cell cycle process. Additionally, MKI67 was highly correlated with TAO. Besides, the DEGs of *GTF2F1*, *SMC3*, *USF1* and *ZNF263* were predicted as transcription factors (TFs).

• **CONCLUSION:** Several crucial genes are identified such as *TPX2*, *CDCA5*, *PRC1* and *KIF23*, which all might play significant roles in TAO via the regulation of cell cycle process. Regulatory relationships between *TPX2* and *CDCA5* as well as between *PRC1* and *KIF23* may exist.

Additionally, MKI67 may be a potent biomarker of TAO, and SMC3 and ZNF263 may exert their roles as TFs in TAO progression.

• **KEYWORDS:** microarray; thyroid associated ophthalmopathy; cell cycle; biomarker

DOI:10.18240/ijo.2018.09.09

Citation: Yang HB, Jiang J, Li LL, Yang HQ, Zhang XY. Biomarker identification of thyroid associated ophthalmopathy using microarray data. *Int J Ophthalmol* 2018;11(9):1482-1488

INTRODUCTION

Graves' disease is a type of autoimmune problem that causes the thyroid gland to produce too much thyroid hormone, which is called hyperthyroidism. Whereas, thyroid associated ophthalmopathy (TAO), also called Graves' orbitopathy, which is closely correlated with Graves' hyperthyroidism (GH), is normally considered as an inflammatory autoimmune eye disorder^[1-2]. Annually, it is reported that 16 of per 100 000 females and 2.9 of per 100 000 males are suffered from TAO^[3]. The current therapeutic strategies were through treating with corticosteroids, external beam radiation or surgery, however, the occurrence of this disease could not be prevented. Previously, the thyrotropin receptor (TSHR) was demonstrated be closely associated with TAO, and it was hypothesized that the progression of ophthalmopathy is the autoimmunity against TSHR in the orbital preadipocyte and extraocular muscle fibroblasts^[4-5]. However, due to the inadequate interpretation for eye muscle swelling and the lack of correlation between TSHR antibody level and eye signs, more appropriate theories are explored by other investigations. Some researchers prefer to stress the significant role of autoimmunity against orbital connective tissue (OCT)^[6] and eye muscle antigens^[7]. Among them, the calcium binding protein calsequestrin was highly over-expressed in eye muscle and was proposed as the causative factor for the orbital skeletal muscle inflammation in TAO^[8]. Further investigation conducted by Lahooti *et al*^[9] suggested that calsequestrin might serve as a candidate in the pathogenesis of TAO. In addition, they also explored the role of the OCT antigen collagen XIII and indicated the serum antibodies against collagen XIII may contribute to the congestive ophthalmopathy^[9]. Multiple inflammation relating biomarkers including *ICAM-1*, *VCAM-1* and

TIMP-1 have been linked to autoimmune thyroid disorders^[10] but only a handful of genetic factors such as *PTPN22*, *TSHR*, *CTLA* and *CD40* as well as *AFF3* and *CD226* were involved in the TAO biomarker establishment^[11].

Recently, a study used microarray analysis to identify differentially expressed genes (DEGs) between GH (thyroid Graves' patients without ophthalmopathy) and TAO. Though the study screened 295 significant DEGs, their emphasis was on the correlation between the most up-regulated cardiac calsequestrin gene (*CASQ2*) and TAO^[12], no more additional relevant genes were elaborated. Therefore, we re-analyzed the microarray data to further explore crucial DEGs between TAO and GH patients without ophthalmopathy, followed by the functional enrichment analysis for the selected DEGs. Moreover, a protein-protein interaction (PPI) network was constructed, from which specific modules are extracted to obtain more exact correlations between the DEGs, attempting to uncover the pathogenesis of TAO and provide potential biomarkers for the prognosis and therapeutic methods of TAO.

SUBJECTS AND METHODS

Microarray Data The expression profile GSE9340, which was deposited in the GEO (Gene Expression Omnibus; <http://www.ncbi.nlm.nih.gov/geo>) database by Wescombe *et al*^[12], included 18 thyroid tissue samples from 10 TAO patients (TAO group) and 8 GH patients without ophthalmopathy (control group). The platform was HumanRef-8 v2 Expression BeadChip.

Ethics Approval and Consent to Participate This study was approved by Ethics Committee of the First Affiliated Hospital of Harbin Medical University and the Second Affiliated Hospital of Harbin Medical University.

Data Preprocessing and the Identification of Differentially Expressed Genes Based on the profiling files, probes were converted to the gene symbols. The probe not corresponding to gene symbols were removed, and when multiple probes corresponded to a single gene, the average level of probes was calculated as the expression value of the specific gene. The raw data were normalized using median method of preprocess Core package^[13]. After the data preprocessing, package limma (Linear Models for Microarray Analysis) of Bioconductor R (<http://www.bioconductor.org/packages/release/bioc/html/limma.html>)^[14] was used to identify the DEGs between TAO and control groups, basing on *t*-test method. The genes met with the criteria of *P* value <0.05 and $|\log_2(\text{fold change})| \geq 1.5$ were considered as DEGs.

Functional Enrichment Analysis The selected DEGs were mapped to gene ontology (GO; <http://www.geneontology.org/>) database to explore their potential process in terms of biological process (BP), molecular function (MF) and cellular component (CC), using the tool of DAVID (Database for

Annotation, Visualization and Integration Discovery; <http://david.abcc.ncifcrf.gov/>)^[15]. Additionally, Kyoto Encyclopedia of Genes and Genomes (KEGG; <http://www.genome.jp/kegg/pathway.html>) enrichment analysis was performed to identify the pathways in which these DEGs might involve. The threshold based on hypergeometric test for significant GO terms and pathways were *P*<0.05.

Protein-protein Interaction Network Construction

Considering that protein encoding by these selected DEGs might exert their functions combining with other proteins, the DEGs were mapped to STRING (Search Tool for the Retrieval of Interacting Genes; <http://string-db.org/>)^[16] database to identify the potential interactions between them and other genes from protein level. The interaction with a combined score >0.7 was screened to establish the PPI network, visualizing by Cytoscape software^[17].

Furthermore, the ClusterOne^[18], a Cytoscape software plugin, was employed to explore the functional modules of the network and subsequently, followed by the GO enrichment analysis for significant modules, using the BiNGO plugin^[19]. The *P* value was adjusted to false discover rate (FDR) and the cut-off value for significant BP terms was FDR<0.05.

Prediction of Transcription Factor and Other Related Genes

Combining the information of transcription factors (TFs) with their targets in University of California Santa Cruz (UCSC) Genome Browser database (<http://genome.ucsc.edu/>)^[20], the TFs among these DEGs were predicted as well as the corresponding targets. Subsequently, Comparative Toxicogenomics Database (CTD; <http://ctdbase.org/>)^[21] was used to identify TAO-related genes among our selected DEGs. The database collects disease-related genes which have been validated by experiment or been reported by literature.

RESULTS

Identification of Differentially Expressed Genes Between Thyroid Associated Ophthalmopathy and Control Groups

Data after normalization exhibited a uniform distribution of the mean value, indicating a favorable normalization that the data were eligible to identify the DEGs. According to the aforementioned criteria, a total of 433 up-regulated and 428 down-regulated DEGs were screened.

Over-represented Processes and Pathways by Enrichment Analysis

With the predefined criteria, correlated processes and pathways which the DEGs might involve in were filtered out. The up-regulated DEGs were predominantly enriched in GO terms such as generation of precursor metabolites and energy (GO:0006091), oxidation reduction (GO:0055114), glycolysis (GO:0006096), mitochondrion (GO:0005739) and 4 iron, 4 sulfur cluster binding (GO:0051539); while the down-regulated DEGs were significantly correlated with cell cycle related processes (GO:0051301, GO:0007049 and GO:0022403) and

Biomarker of TAO

regulation of transcription (GO:0045449) (Table 1). KEGG enrichment analysis indicated that the over-presented pathways for the up-regulated DEGs were fructose and mannose metabolism, protein export and citrate cycle, whereas the down-regulated DEGs were mainly enriched in systemic lupus erythematosus, oocyte meiosis and progesterone-mediated oocyte maturation (Table 2).

Constructed Protein-protein Interaction Network of the Differentially Expressed Genes and the Module Analysis

By mapping the protein information in STRING database, a PPI network was established for the protein products of the DEGs, embracing 696 interactions and 339 nodes. A protein in the PPI network was defined as a “node” and the “degree” of the node referred to the interaction number of that particular protein. The most highly connected nodes with high degree were deemed as the “hubs” of the network. The remarkable hubs in the PPI network were presented in Figure 1, embracing BUB1B (degree=35), CDC20 (degree=33), CDCA8 (degree=26), PRC1 (degree=24), CENPA (degree=24), CCNB2 (degree=24), TPX2 (degree=23), CDCA5 (degree=23), KIF23 (degree=23) and SPC25 (degree=23).

Using the ClusterOne plugin, a significant module was extracted from the PPI network, involving 236 interactions and 27 nodes, in which the nodes with high degrees were highlighted including SPC25 (degree=23), TPX2 (degree=23), CENPA (degree=23), KIF23 (degree=22), PRC1 (degree=22), CDCA5 (degree=21), HMMR (degree=21), KIF20A (degree=21), RAD51AP1 (degree=21) and MKI67 (degree=19) (Figure 2). In addition, there were some interactions between these hub protein pairs, such as TPX and KIF23 or MKI67 or PRC1, MKI67 and PRC1 or KIF23 or CDCA5, as well as CDCA5 and KIF23. The functional enrichment for genes in the module was performed by the BinGO plugin. As presented in Table 3, genes which encoded the predominant nodes in the module (such as *KIF23*, *TPX2*, *MKI67*, *PRC1* and *CDCA5*) were mainly correlated with the processes related to cell division and cell cycle.

Predicted Transcription Factors As a result, a total of 88 TFs involving 4700 targeting interactions were predicted through the comparison with the TFs in UCSC database. Among them, four TFs were encoded by DEGs such as *GTF2F1*, *SMC3*, *USF1* and *ZNF263*, in which *SMC3* was up-regulated, while others were down-regulated. The targets of the four TFs were revealed in Figure 3.

Thyroid Associated Ophthalmopathy Related Genes We obtained 1406 genes associated with TAO from CTD database, including 42 DEGs in the present study (Table 4). In other words, these DEGs were prominent in TAO pathogenesis. Notably, the down-regulated *MKI67* with a high degree of 19, which was a hub protein in the module, was highly associated with TAO.

Table 1 Significant enriched GO terms of up- and down-regulated DEGs in thyroid-associated ophthalmopathy (top 5 ranked by *P* value)

Category	Count	<i>P</i>
Up-regulated DEGs		
BP		
GO:0006091 (generation of precursor metabolites and energy)	20	6.94E-05
GO:0055114 (oxidation reduction)	31	8.20E-05
GO:0006096 (glycolysis)	6	0.003661203
GO:0003012 (muscle system process)	11	0.004182103
GO:0006614 (SRP-dependent cotranslational protein targeting to membrane)	3	0.006886459
CC		
GO:0005739 (mitochondrion)	43	4.40E-04
GO:0044429 (mitochondrial part)	25	0.004604374
GO:0005625 (soluble fraction)	16	0.005293665
GO:0005829 (cytosol)	45	0.00664855
GO:0005786 (signal recognition particle, endoplasmic reticulum targeting)	3	0.00724437
MF		
GO:0051539 (4 iron, 4 sulfur cluster binding)	6	2.66E-04
GO:0050662 (coenzyme binding)	14	3.94E-04
GO:0048037 (cofactor binding)	16	9.28E-04
GO:0001882 (nucleoside binding)	58	0.001301458
GO:0050660 (FAD binding)	8	0.001584685
Down-regulated DEGs		
BP		
GO:0045449 (regulation of transcription)	97	5.83E-08
GO:0006350 (transcription)	81	3.39E-07
GO:0051301 (cell division)	22	2.51E-06
GO:0007049 (cell cycle)	38	7.99E-06
GO:0022403 (cell cycle phase)	25	1.65E-05
CC		
GO:0043228 (non-membrane-bounded organelle)	86	4.24E-06
GO:0043232 (intracellular non-membrane-bounded organelle)	86	4.24E-06
GO:0015630 (microtubule cytoskeleton)	28	3.02E-05
GO:0005819 (spindle)	13	5.71E-05
GO:0031981 (nuclear lumen)	51	2.12E-04
MF		
GO:0016564 (transcription repressor activity)	22	7.25E-06
GO:0003677 (DNA binding)	76	3.15E-04
GO:0030528 (transcription regulator activity)	52	0.001310177
GO:0016566 (specific transcriptional repressor activity)	5	0.007895981
GO:0016702 (oxidoreductase activity, acting on single donors with incorporation of molecular oxygen, incorporation of two atoms of oxygen)	6	0.015210301

GO: Gene ontology; DEG: Differentially expressed genes; Count: Number of the DEGs in a specific term; BP: Biological process; MF: Molecular function; CC: Cellular components.

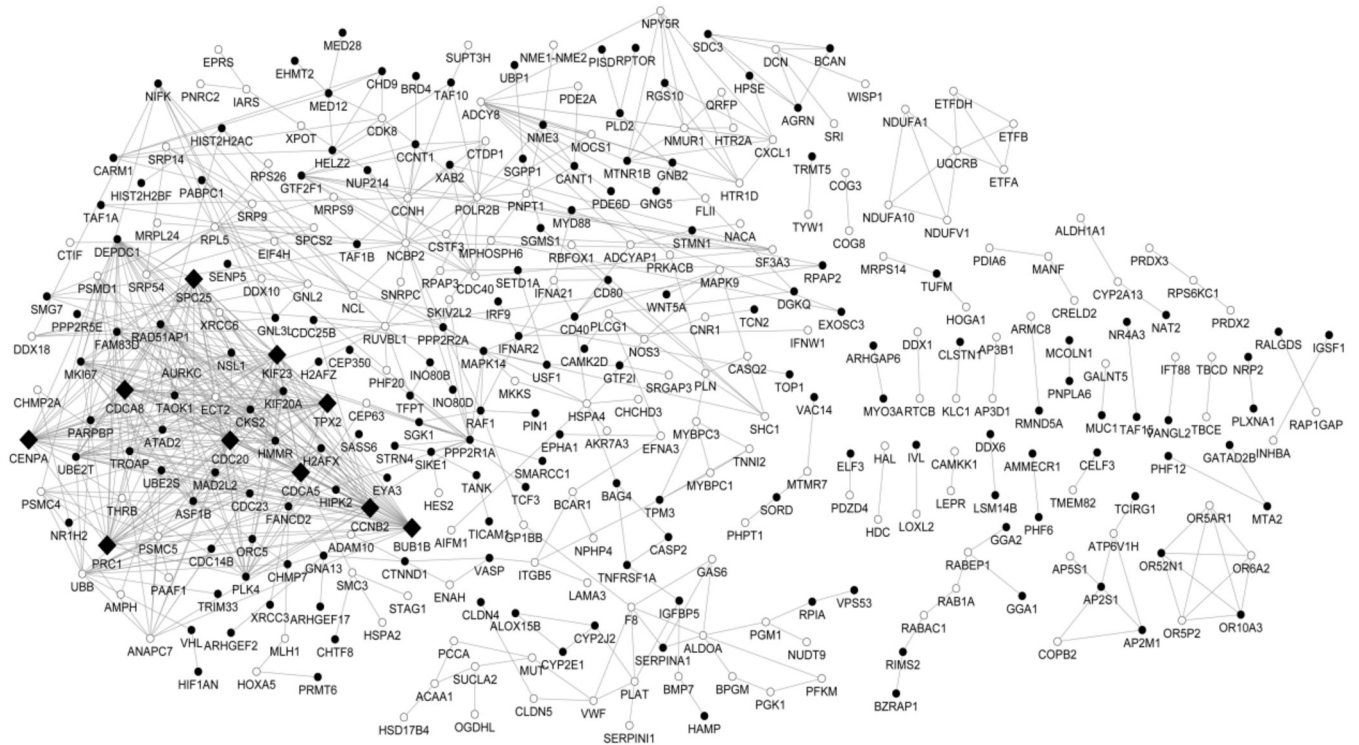


Figure 1 Protein-protein interaction network of the DEGs The white round represents proteins encoded by up-regulated DEGs and the black round represents proteins encoded by down-regulated DEGs. The protein products in the networks serve as the “nodes”, and the undirected link denotes each pairwise interaction. The most highly connected nodes with high degree were deemed as the “hubs”. In the network, the black rhombus indicates hub proteins.

Table 2 Significant enriched pathways for up- and down-regulated DEGs

Items	Gene	P
Up-regulated DEGs		
hsa00051: Fructose and mannose metabolism	<i>ALDOA, GMDS, PFKM, MTMR7, PHPT1</i>	0.011005787
hsa03060: Protein export	<i>SRP14, SRP54, SRP9</i>	0.016901464
hsa00020: Citrate cycle (TCA cycle)	<i>SDHA, ACO2, OGDHL, SUCLA2</i>	0.045286512
Down-regulated DEGs		
hsa05322: Systemic lupus erythematosus	<i>CD80, HIST2H2AC, HIST2H2BF, HIST1H2BH, H2AFZ, H2AFX, H2AFJ, CD40</i>	0.005051127
hsa04114: Oocyte meiosis	<i>PPP2R1A, CCNB2, CAMK2D, CDC23, CDC20, PPP2R5E, MAD2L2</i>	0.029954967
hsa04914: Progesterone-mediated oocyte maturation	<i>CCNB2, MAPK14, CDC23, RAF1, MAD2L2, CDC25B</i>	0.036489027

DEG: Differentially expressed genes.

Table 3 Enrichment analysis for genes in the module

Terms	P	FDR	Genes
GO:0051301 (cell division)	8.80E-16	2.78E-13	<i>FAM83D, KIF23, SPC25, CDCA8, CCNB2, PRC1, NSL1, CKS2, TPX2, AURKC, BUB1B, CDC20, CDCA5</i>
GO:0000279 (M phase)	3.74E-15	5.90E-13	<i>FAM83D, KIF23, SPC25, CDCA8, CCNB2, MKI67, PRC1, NSL1, CKS2, TPX2, BUB1B, CDC20, CDCA5</i>
GO:00022403 (cell cycle phase)	5.94E-14	6.25E-12	<i>FAM83D, KIF23, SPC25, CDCA8, CCNB2, MKI67, PRC1, NSL1, CKS2, TPX2, BUB1B, CDC20, CDCA5</i>
GO:00022402 (cell cycle process)	8.60E-14	6.80E-12	<i>FAM83D, KIF23, SPC25, CDCA8, CCNB2, MKI67, PRC1, CENPA, NSL1, CKS2, TPX2, BUB1B, CDC20, CDCA5</i>
GO:0007049 (cell cycle)	2.49E-13	1.58E-11	<i>KIF23, PRC1, MKI67, AURKC, TPX2, CDC20, FAM83D, SPC25, CDCA8, CCNB2, CENPA, NSL1, CKS2, BUB1B, CDCA5</i>
GO:0000278 (mitotic cell cycle)	3.96E-13	2.08E-11	<i>FAM83D, KIF23, SPC25, CDCA8, CCNB2, PRC1, CENPA, NSL1, TPX2, BUB1B, CDC20, CDCA5</i>
GO:0007067 (mitosis)	2.74E-12	1.08E-10	<i>FAM83D, KIF23, SPC25, CDCA8, CCNB2, NSL1, TPX2, BUB1B, CDC20, CDCA5</i>
GO:0000280 (nuclear division)	2.74E-12	1.08E-10	<i>FAM83D, KIF23, SPC25, CDCA8, CCNB2, NSL1, TPX2, BUB1B, CDC20, CDCA5</i>
GO:0000087 (M phase of mitotic cell cycle)	3.68E-12	1.26E-10	<i>FAM83D, KIF23, SPC25, CDCA8, CCNB2, NSL1, TPX2, BUB1B, CDC20, CDCA5</i>
GO:0048285 (organelle fission)	4.00E-12	1.26E-10	<i>FAM83D, KIF23, SPC25, CDCA8, CCNB2, NSL1, TPX2, BUB1B, CDC20, CDCA5</i>

GO: Gene ontology; FDR: False discovery rate.

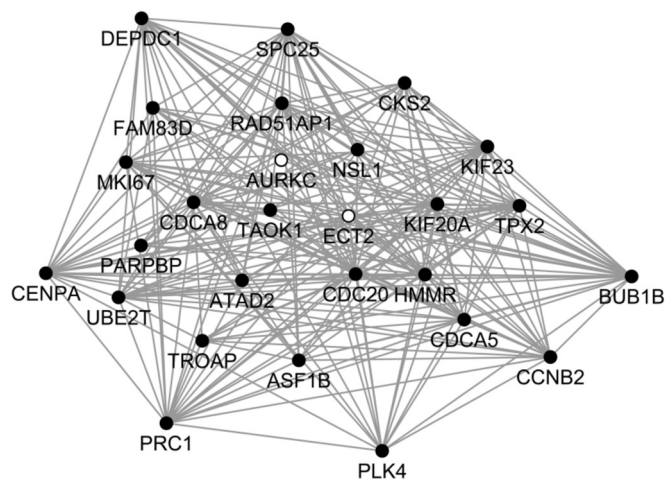


Figure 2 Module of the DEGs The white round represents proteins encoded by up-regulated DEGs and the black represents proteins encoded by down-regulated DEGs. The protein products in the networks serve as the 'nodes', and the undirected link denotes each pairwise interaction.

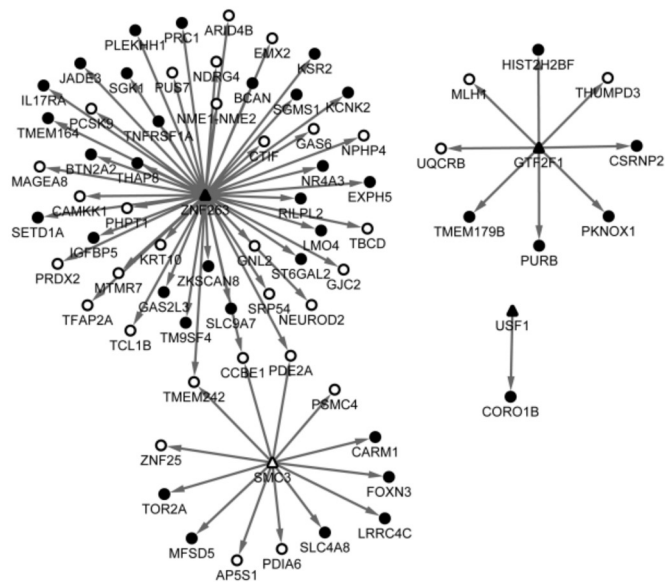


Figure 3 Predicted targets of the TFs The triangle represents TF and the round represents the targets, in which the white denotes up-regulated and the black denotes down-regulated. The arrow indicates the relationships between TFs and the targets.

DISCUSSION

As a result, a total of 861 DEGs (433 were up-regulated and 428 were down-regulated) between TAO and control groups were identified. Crucial nodes in the PPI network included TPX2, CDCA5, PRC1, KIF23 and MKI67, which were also highlighted in the module of the network and all enriched in cell cycle related processes. Additionally, MKI67 was highly correlated with TAO. Besides, the DEGs of *GTF2F1*, *SMC3*, *USF1* and *ZNF263* were predicted as TFs.

TPX2 (Targeting Protein for the Xenopus kinesin-like protein 2) is essential for normal spindle assembly and meiotic divisions, and also is cell cycle-mediated in somatic cells^[22]. During the stage of meiotic divisions in mouse oocytes, *TPX2* is a

Table 4 The common DEGs (degree>2) based on the genes associated with TAO from CTD database

Genes	Degree
<i>MKI67</i>	19
<i>UBB</i>	17
<i>PPP2R1A</i>	14
<i>CXCL1</i>	7
<i>F8</i>	6
<i>UQCRB</i>	6
<i>CD40</i>	6
<i>PLAT</i>	5
<i>DCN</i>	5
<i>VWF</i>	4
<i>IFNAR</i>	4
<i>AGR2</i>	4
<i>TPM3</i>	4
<i>NOS3</i>	4
<i>NDUFA10</i>	3
<i>NDUFA1</i>	3
<i>NDUFV1</i>	3
<i>SUCLA2</i>	3
<i>ETFDH</i>	3
<i>ETFA</i>	3
<i>MUT</i>	3
<i>ACAA1</i>	3
<i>ETFB</i>	3

central target of Ran, the active form of which (Ran-GTP) was essential for mitotic spindles organization^[23]. By interacting with the Kinesin-5 motor Eg5, another spindle-associated protein, TPX2 was demonstrated to facilitate to the localization of Eg5 to spindle microtubules with the bacterial artificial chromosome method^[24]. *CDCA5* (cell division cycle associated 5) is another cell cycle associated gene which mainly serves as a regulator of sister chromatid cohesion in mitosis stabilizing cohesin complex. The human breast cancer-associated fibroblast genes including *CDCA5* and *TRIP13* (thyroid hormone receptor interactor 13), which played significant roles in chromosome recombination and chromosome structure development during meiosis, were enriched in cell cycle BP function^[25]. Though there were rare evidence that validated the relationships between *TPX2* and *CDCA5* especially in TAO disease, a study using genome-scale RNAi profiling technique indicated that both *TPX2* and *CDCA5* (*KIF20A*) were associated with cell division phenotypes^[26]. In the present study, as two vital nodes in the module of the network, *CDCA5* and *TPX2* were both enriched in mitotic cell cycle function, and notably, *CDCA5* was linked to *TPX2*, providing a hint that the dysfunction in mitotic cell cycle process, which might be mediated by the interaction of *TPX2* and *CDCA5*, might play important roles in the TAO associated events.

PRC1 and KIF23 were another two remarkable nodes as revealed in the module. The protein encoded by *PRC1* is a central-spindle matrix protein and involved in cytokinesis^[27-28]. The absence of *PRC1* could result in the disorganization of motor protein. Besides, it was convinced that PRC1 was required in the MKlp1 (the kinesin-6 family motor protein) mediated targeting to the central spindle^[29]. As a kinesin-like protein family member, KIF23 is also involved in cell division. Notably, the protein KIF23 serves as a part of the central spindle, which exhibited at the spindle midzone as a complex of PRC1 and AURKB (aurora kinase B), to regulate the central spindle assembly in endometrial cancers^[30]. As expected, our functional enrichment results indicated that both of *PRC1* and *KIF23* were closely related to cell cycle associated processes such as mitotic cell cycle, nuclear division and M phase of mitotic cell cycle, which might support the hypothesis that *PRC1* and *KIF23* might exert significant roles in TAO *via* the cell cycle mediated regulation. What's more, KIF23 was linked to PRC1 in the module, suggesting a potential regulatory relationship might exist between these two encoded genes.

MKI67 encodes a nuclear protein that is highly associated with cellular proliferation. Furthermore, this gene has even been used as a cell cycle marker for the prognosis of various diseases including Alzheimer disease^[31] and hepatocellular carcinoma^[32]. Interestingly, *MKI67* is implied in the TAO disease *via* the interactions with chemicals such as peroxisome proliferator activated receptor- γ (PPAR- γ) and thiazolidinediones (TZDs), which were closely linked to TAO^[33]. This provided a clue that *MKI67* might be a potent biomarker of TAO detection.

Four crucial DEGs including *SMC3* (structural maintenance of chromosomes 3) and *ZNF263* were identified as TFs related to TAO. The gene *SMC3* was also cell cycle related. The nuclear form of the *SMC3* encoded protein is an essential element for the cohesion of sister chromatids during mitosis. Besides, the *SMC3* acetylation is the basic mechanism in the regulation of sister chromatid cohesion^[34]. Recruiting the method of logistic regression classifiers, *SMC3* was observed implicated in the G2/M stage of the cell cycle^[35]. In the present study, *SMC3* was predicted as a TF correlated with TAO, implying that *SMC3* might regulate other genes expression *via* the direct targeting. Unfortunately, rare evidence was existed to reveal the *SMC3*'s role as a TF, nor the corresponding targets. Therefore, our findings might provide a new insight into the role of *SMC3* with regard to TAO. The *ZNF263* (zinc finger protein 263) was generally considered to have an important role in basic cellular processes as a transcriptional repressor, but a recent study discovered that though embracing the KRAB domain which contributed to transcriptional repressor, the targets of *ZNF263* had a high expression level, and the researchers proposed that *ZNF263* might exert both positive and negative regulation of

its targets as a TF^[36]. Likewise, there was any studies reported the role of *ZNF263* as a TF with regard to TAO but our results indicated that *ZNF263* was a critical DEG and meanwhile was predicted as a TF related to TAO, implying it might have important roles in TAO events through the transcriptional regulation of its targets.

However, these are some limitations in our study. For examples, there are no enough samples from patients and have not been collected at present. In addition, there are also no suitable cell lines at present. Although all of the predicted results should be confirmed by laboratory data, the findings might provide a scientific guidance for future study and improve a further understanding of the progression of TAO.

In conclusion, our results identified several crucial genes related to TAO including *TPX2*, *CDCA5*, *PRC1* and *KIF23*, which all might involve in cell cycle related process. Furthermore, regulatory relationships between *TPX2* and *CDCA5* as well as between *PRC1* and *KIF23* might exist. Additionally, *MKI67* might be a potent biomarker of TAO, and *SMC3* and *ZNF263* might exert their roles as TFs in TAO progression.

ACKNOWLEDGEMENTS

Authors' contributions: Conception and design of the research: Yang HB; Acquisition of data: Jiang J; Analysis and interpretation of data: Li LL; Statistical analysis: Yang HQ and Zhang XY; Drafting the manuscript: Yang HB; Revision of manuscript for important intellectual content: Yang HB and Jiang J.

Conflicts of Interest: Yang HB, None; Jiang J, None; Li LL, None; Yang HQ, None; Zhang XY, None.

REFERENCES

- 1 Maheshwari R, Weis E. Thyroid associated orbitopathy. *Indian J Ophthalmol* 2012;60(2):87-93.
- 2 Gopinath B, Wescombe L, Nguyen B, Wall JR. Can autoimmunity against caldesmon explain the eye and eyelid muscle inflammation of thyroid eye disease? *Orbit* 2009;28(4):256-261.
- 3 Gould DJ, Roth FS, Soparkar CN. The diagnosis and treatment of thyroid-associated ophthalmopathy. *Aesthetic Plast Surg* 2012;36(3): 638-648.
- 4 Bahn RS. Clinical review 157: pathophysiology of Graves' ophthalmopathy: the cycle of disease. *J Clin Endocrinol Metab* 2003;88(5):1939-1946.
- 5 Boschi A. Quantification of cells expressing the thyrotropin receptor in extraocular muscles in thyroid associated orbitopathy. *Br J Ophthalmol* 2005;89(6):724-729.
- 6 Lehmann GM, Feldon SE, Smith TJ, Phipps RP. Immune mechanisms in thyroid eye disease. *Thyroid* 2008;18(9):959-965.
- 7 Tani J, Wall JR. Autoimmunity against eye-muscle antigens may explain thyroid-associated ophthalmopathy. *CMAJ* 2006;175(3):239.
- 8 Porter JD, Khanna S, Kaminski HJ, Rao JS, Merriam AP, Richmonds CR, Leahy P, Li J, Andrade FH. Extraocular muscle is defined by a fundamentally distinct gene expression profile. *Proc Natl Acad Sci U S A* 2001;98(21):12062-12067.

- 9 Lahooti H, Parmar KR, Wall JR. Pathogenesis of thyroid-associated ophthalmopathy: does autoimmunity against calsequestrin and collagen XIII play a role? *Clin Ophthalmol* 2010;4(1):417-425.
- 10 Jublanc C, Beaudoux JL, Aubart F, Raphael M, Chadarevian R, Chapman MJ, Bonnefont-Rousselot D, Bruckert E. Serum levels of adhesion molecules ICAM-1 and VCAM-1 and tissue inhibitor of metalloproteinases, TIMP-1, are elevated in patients with autoimmune thyroid disorders: relevance to vascular inflammation. *Nutr Metab Cardiovasc Dis* 2011;21(10):817-822.
- 11 Płoski R, Szymański K, Bednarczuk T. The genetic basis of Graves' disease. *Curr Genomics* 2011;12(8):542-563.
- 12 Wescombe L, Lahooti H, Gopinath B, Wall JR. The cardiac calsequestrin gene (CASQ2) is up-regulated in the thyroid in patients with Graves' ophthalmopathy-support for a role of autoimmunity against calsequestrin as the triggering event. *Clin Endocrinol* 2010;73(4):522-528.
- 13 Bolstad B. Preprocessscore: A collection of pre-processing functions. R package, version 1.20. 0. 2010
- 14 Smyth GK. Limma: linear models for microarray data. *Bioinformatics and computational biology solutions using R and bioconductor*. Germany: Springer; 2005:397-420.
- 15 Dennis G Jr, Sherman BT, Hosack DA, Yang J, Gao W, Lane HC, Lempicki RA. DAVID: Database for annotation, visualization, and integrated discovery. *Genome Biol* 2003;4(5):P3.
- 16 Szklarczyk D, Franceschini A, Kuhn M, Simonovic M, Roth A, Minguez P, Doerks T, Stark M, Muller J, Bork P, Jensen LJ, von Mering C. The STRING database in 2011: functional interaction networks of proteins, globally integrated and scored. *Nucleic Acids Res* 2011;39(Database issue):D561-D568.
- 17 Smoot ME, Ono K, Ruscheinski J, Wang PL, Ideker T. Cytoscape 2.8: new features for data integration and network visualization. *Bioinformatics* 2010;27(3):431-432.
- 18 Nepusz T, Yu H, Paccanaro A. Detecting overlapping protein complexes in protein-protein interaction networks. *Nat Methods* 2012;9(5):471-472.
- 19 Maere S, Heymans K, Kuiper M. BiNGO: a cytoscape plugin to assess overrepresentation of gene ontology categories in biological networks. *Bioinformatics* 2005;21(16):3448-3449.
- 20 Karolchik D, Barber GP, Casper J, et al. The ucsc genome browser database: 2014 update. *Nucleic Acids Res* 2014;42(Database issue): D764-D770.
- 21 Davis AP, Murphy CG, Johnson R, Lay JM, Lennon-Hopkins K, Saraceni-Richards C, Sciaky D, King BL, Rosenstein MC, Wieggers TC, Mattingly CJ. The comparative toxicogenomics database: update 2013. *Nucleic Acids Res* 2013;41(Database issue):D1104-D1114.
- 22 Brunet S, Dumont J, Lee KW, Kinoshita K, Hikal P, Gruss OJ, Maro B, Verlhac MH. Meiotic regulation of TPX2 protein levels governs cell cycle progression in mouse oocytes. *PLoS One* 2008;3(10):e3338.
- 23 Gruss OJ, Vernos I. The mechanism of spindle assembly functions of Ran and its target TPX2. *J Cell Biol* 2004;166(7):949-955.
- 24 Ma N, Titus J, Gable A, Ross JL, Wadsworth P. TPX2 regulates the localization and activity of Eg5 in the mammalian mitotic spindle. *J Cell Biol* 2011;195(1):87-98.
- 25 Mercier I, Casimiro MC, Wang C, et al. Human breast cancer-associated fibroblasts (CAFs) show caveolin-1 down-regulation and RB tumor suppressor functional inactivation: Implications for the response to hormonal therapy. *Cancer Biol Ther* 2008;7(8):1212-1225.
- 26 Kittler R, Pelletier L, Heninger AK, et al. Genome-scale RNAi profiling of cell division in human tissue culture cells. *Nat Cell Biol* 2007;9(12):1401-1412.
- 27 Shrestha S, Wilmeth LJ, Eyer J, Shuster CB. PRC1 controls spindle polarization and recruitment of cytokinetic factors during monopolar cytokinesis. *Mol Biol Cell* 2012;23(7):1196-1207.
- 28 Subramanian R, Ti SC, Tan L, Darst SA, Kapoor TM. Marking and measuring single microtubules by PRC1 and kinesin-4. *Cell* 2013;154(2):377-390.
- 29 Neef R, Klein UR, Kopajtich R, Barr FA. Cooperation between mitotic kinesins controls the late stages of cytokinesis. *Curr Biol* 2006;16(3):301-307.
- 30 Chou WC, Cheng AL, Brotto M, Chuang CY. Visual gene-network analysis reveals the cancer gene co-expression in human endometrial cancer. *BMC Genomics* 2014;15:300.
- 31 Bonda DJ, Lee HP, Kudo W, Zhu X, Smith MA, Lee HG. Pathological implications of cell cycle re-entry in Alzheimer disease. *Expert Rev Mol Med* 2010;12:e19.
- 32 Hou YY, Cao WW, Li L, Li SP, Liu T, Wan HY, Liu M, Li X, Tang H. MicroRNA-519d targets MKi67 and suppresses cell growth in the hepatocellular carcinoma cell line QGY-7703. *Cancer Lett* 2011;307(2): 182-190.
- 33 Lee S, Tsirbas A, Goldberg RA, McCann JD. Thiazolidinedione induced thyroid associated orbitopathy. *BMC Ophthalmol* 2007; 7(1):8.
- 34 Zhang J, Shi X, Li Y, et al. Acetylation of SMC3 by Eco1 is required for S phase sister chromatid cohesion in both human and yeast. *Mol Cell* 2008;31(1):143-151.
- 35 Ernst J, Plasterer HL, Simon I, Bar-Joseph Z. Integrating multiple evidence sources to predict transcription factor binding in the human genome. *Genome Res* 2010;20(4):526-536.
- 36 Fretze S, Lan X, Jin VX, Farnham PJ. Genomic targets of the KRAB and SCAN domain-containing zinc finger protein 263. *J Biol Chem* 2010;285(2):1393-1403.